SUPPLEMENTAL MATERIAL

Methods

Virus production: TET2 shRNA retroviruses and TET2 over-expressing lentiviruses were generated using standard protocols. Plasmids were transfected into HEK293 cells using Fugene 6, and the viral supernatant collected by ultracentrifugation. Viruses were titered using published methods.[1, 2] The TET2 adenovirus was purchased from Welgen, Inc. (Worcester, MA). TET2 knockdown cells were collected 48 hours post-infection. Cells were infected with the TET2 overexpression virus for 48 hours prior to puromycin selection for 7-10 days. Efficiency of knockdown and overexpression of TET2 was assessed by qPCR and western blots.

Immunocytochemistry and immunofluorescence: Cells and tissues were fixed and stained using standard protocol. Samples were incubated with antibodies against TET2 (1:250, Sigma-Aldrich), 5-hmC (1:5000, Active Motif), MYH11 (SM-MHC) (1:1000, Abcam), ACTA2 (SM-α-actin) (1:500, Sigma), CDH5 (VE Cadherin) (1:500, Santa Cruz), CD31 (1:400, BD Pharmingen), CD68 (1:400, AbD Serotec), CD45 (1:400, BD Pharmingen). Images were taken using a Nikon A1 spectral confocal laser scanning microscope.

Quantitative morphometry: Tissue morphology was visualized by elastic-Van Gieson (EVG) staining. The areas within the lumen and the areas circumscribed by the internal elastic lamina (IEL) and external elastic lamina (EEL) were determined by tracing along the respective vessel regions. The media was defined as the region between the EEL and the IEL, and the neointima was measured as the region between the lumen and the IEL. Each slide consisted of six sections that were cut 50 μm apart, covering 300 μm of the vessel length. Two or more slides (12-18 sections) per subject were analyzed using a Nikon i80 microscope. Multiple measures in the same subject had high concordance (i.e. intra-class correlation coefficient near 1). The intra-class

correlation coefficient of the same rater single measure reliability ranged from 0.9566 to 0.9914 in the animal studies and was 0.9476 in the clinical study.

qPCR: Total RNA was extracted from cells using the RNeasy mini kit (Qiagen). cDNA was prepared using the SsoFast first strand cDNA synthesis kit (Bio-Rad) and PCR was performed with SYBR green PCR master mix (Bio-Rad). All samples were run in triplicate, from at least three independent experiments, and normalized to *β-actin*. RNA isolation from tissue slides was performed using the Pinpoint™ Slide RNA Isolation System II (Zymo Research) following the manufacturer's instructions. Six sections per mouse were used for analysis, and samples were run in triplicate and normalized to *β-actin.* Primer sequences are listed in Supplementary Table 1-2.

Western blotting: Cell lysates and tissues were lysed with RIPA buffer. Primary antibody used included β-tubulin (1:1000, Santa Cruz), TET1 (1:500, Abcam), TET2 (1:500, Abcam), TET3 (1:500, Abcam), SRF (1:500, Abcam), MYH11 (1:1000, Abcam), ACTA2 (1:500, Abcam), KLF4 (1:1000, Abcam), KLF5 (1:1000, Abcam), OPN (1:1000 Abcam), MYH10 (1:1000, Abcam), CNN1 (1:1000, Sigma), CDH5 (1:500, Santa Cruz). Samples were collected from at least three independent experiments.

*Flow Cytometry***:** Cells were resuspended in PBS and fixed overnight at 4°C with 70% ethanol. The cells were stained with propidium iodide containing RNaseA 1 h prior to analysis. Flow cytometry was performed using BD LSR II flow cytometer and analyzed using FlowJo.

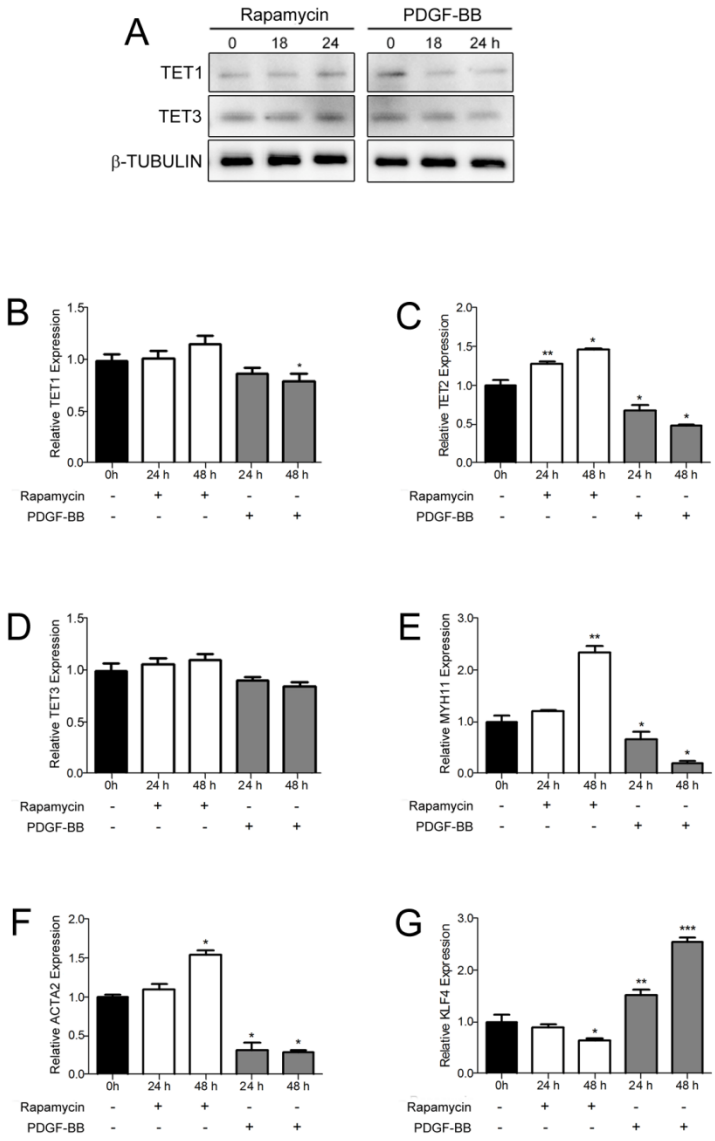

Supplementary Figure 1: TET expression during SMC phenotypic modulation

(A) Western blot of TET1 and TET3 levels in hCASMC treated with 50 nM rapamycin or 5 ng/ml PDGF-BB. **(B-H)** qPCR analyses of *TET1/2/3*, *MYH11*, *ACTA2* and *KLF4* expression in hCASMC treated with 50 nM rapamycin or 5 ng/ml PDGF-BB. All data were normalized to *β*-

actin. Error bars represent mean ± SD for three independent experiments. $^{*}P<0.05$, $^{**}P<0.01$ $^{***}P<0.001$.

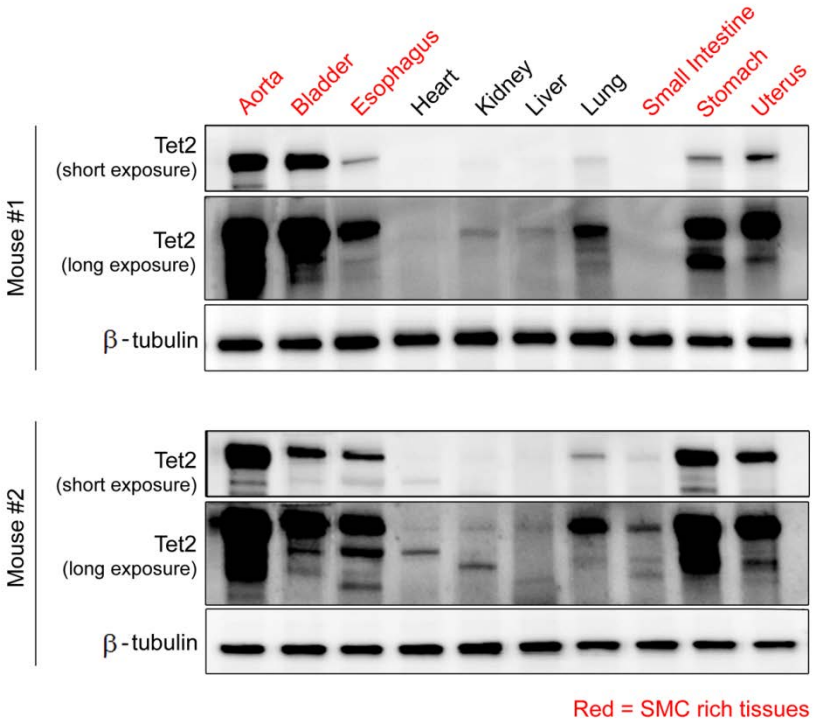

Supplementary Figure 2: TET2 expression is high in SMC-rich tissues

Protein lysates were prepared from 10 different tissues from two mice and levels of Tet2 expression were examined by Western blot.

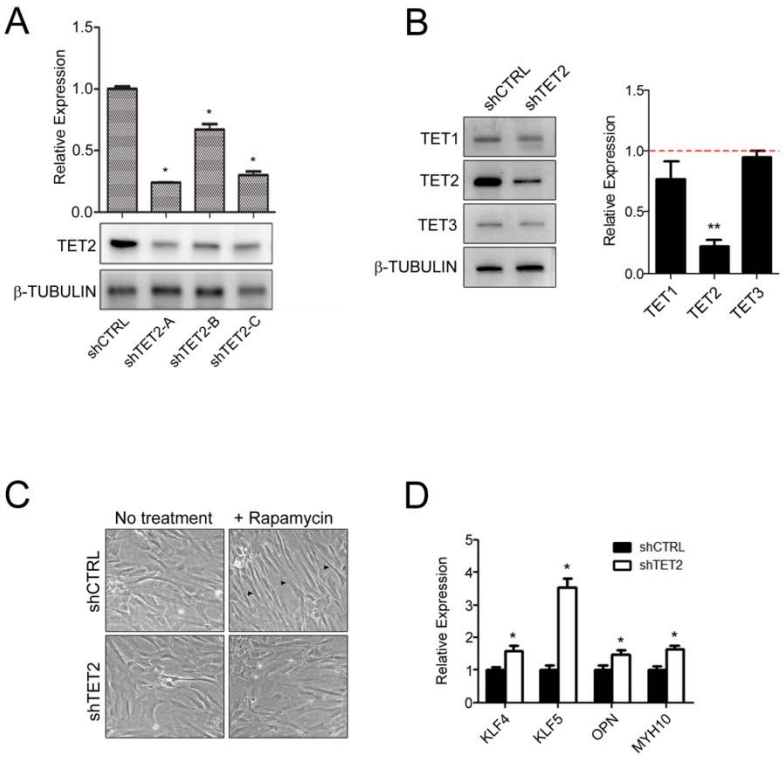

Supplementary Figure 3: Disruption of TET2 results in impaired SMC differentiation and promotes a dedifferentiated phenotype

(A) TET2 protein levels following knockdown using three different constructs in hCASMC, $^{*}P<0.05$ compared to shCTRL. **(B)** Western blot and qPCR demonstrating that TET2 knockdown does not affect TET1 or TET3 expression. Expression was normalized to hESC, denoted at 1.0 by the dotted line. **(C)** Contractile morphology (denoted by arrowheads in shCTRL cells treated with rapamycin) is absent in shTET2 cells after 48 h treatment with 50 nM rapamycin. **(D)** qPCR analysis for the expression of dedifferentiation-associated mRNAs following TET2 knockdown. Data normalized to *β-actin* and represent mean ± SD from three independent knockdown experiments. $^{*}P<0.05$ relative to shCTRL.

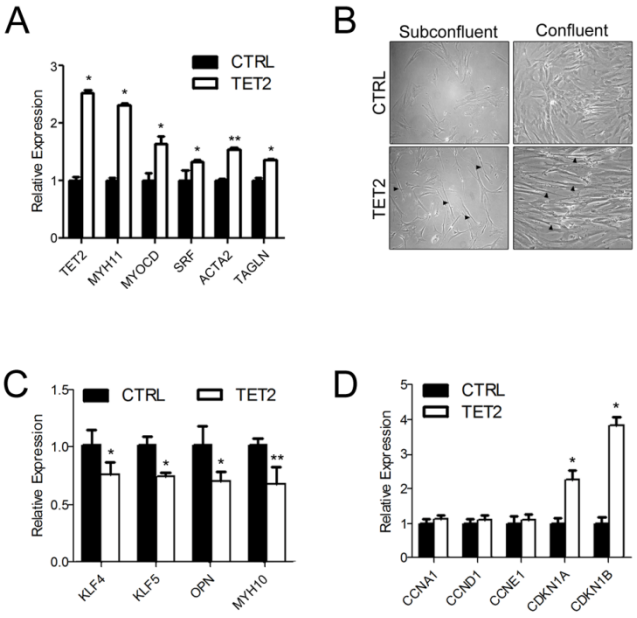

Supplementary Figure 4: TET2 overexpression promotes SMC differentiation

(A) mRNA levels showing *TET2*, *SRF*, *MYOCD* and smooth muscle contractile gene expression in CTRL and TET2 overexpressing hCASMC. **(B)** Phase contrast microscopy showing morphology of control and TET2 overexpressing hCASMC. An elongated morphology (indicated by the arrowheads) characteristic of differentiated SMC was observed with TET2 overexpression. **(C)** mRNA levels of SMC dedifferentiation genes in TET2 overexpressing hCASMC compared to controls. **(D)** mRNA levels of cyclins and cyclin-dependent kinase inhibitors with TET2 overexpression in hCASMC. All qPCR data were normalized to *β-actin* and are presented as mean ± SD from three independent overexpression experiments, $^{*}P<0.05$, $^{**}P<0.01$, $^{***}P<0.001$ relative to CTRL.

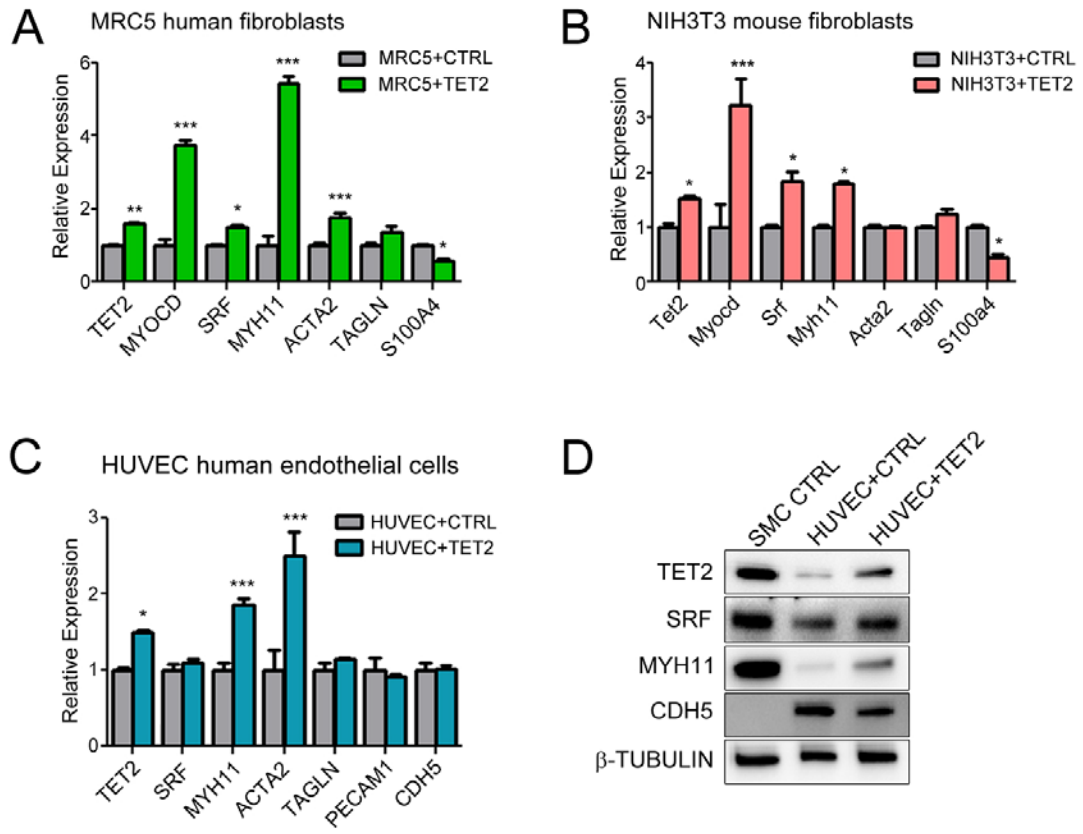

Supplementary Figure 5: Ectopic expression of TET2 directs smooth muscle cell differentiation

qPCR of *TET2*, smooth muscle contractile and fibroblast-specific gene expression in MRC5 human MRC5 **(A)** and NIH3T3 mouse **(B)** fibroblasts infected with the TET2 overexpression virus. **(C)** qPCR of TET2, smooth muscle contractile and endothelial cell specific gene expression in HUVEC cells infected with the TET2 overexpressing virus. **(D)** Western blot of TET2, SRF, MYH11 and CDH5 of TET2 infected HUVEC. All qPCR data were normalized to *β-actin*. Data are presented as mean ± SD. Data shown in **(A)** is representative of four independent experiments. Data shown in **(B-D)** are representatives of three independent repeats. $^{*}P<0.05$, $^{**}P<0.01$, $^{***}P<0.001$ relative to CTRL. Cells were infected with the TET2 overexpressing virus for 2 days and then stably selected with puromycin treatment for 7 days.

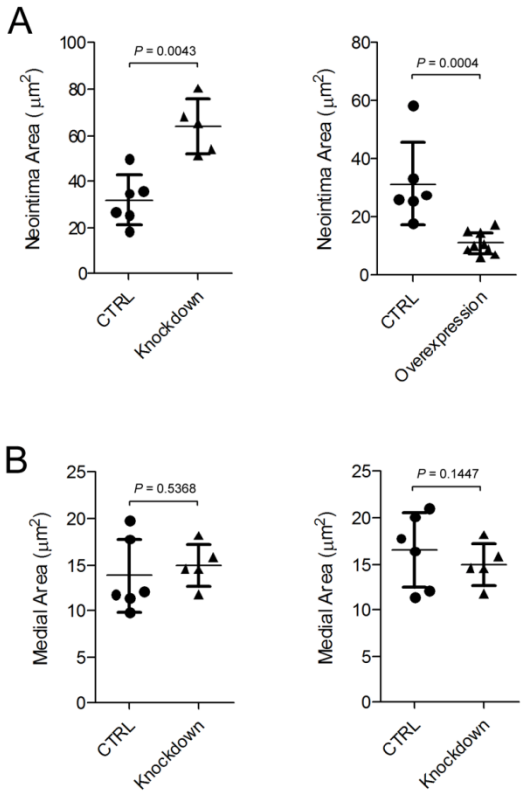

Supplementary Figure 6: Morphometric analysis of TET2 knockdown and overexpression following femoral artery wire injury.

Quantification of neointimal **(A)** and medial **(B)** areas from each group in Figure 5 using computer-assisted image analysis as in Methods. Sample numbers are as in Figure 5B. Six to eight sections from each individual mouse were used for calculations. Data are presented as mean ± SD.

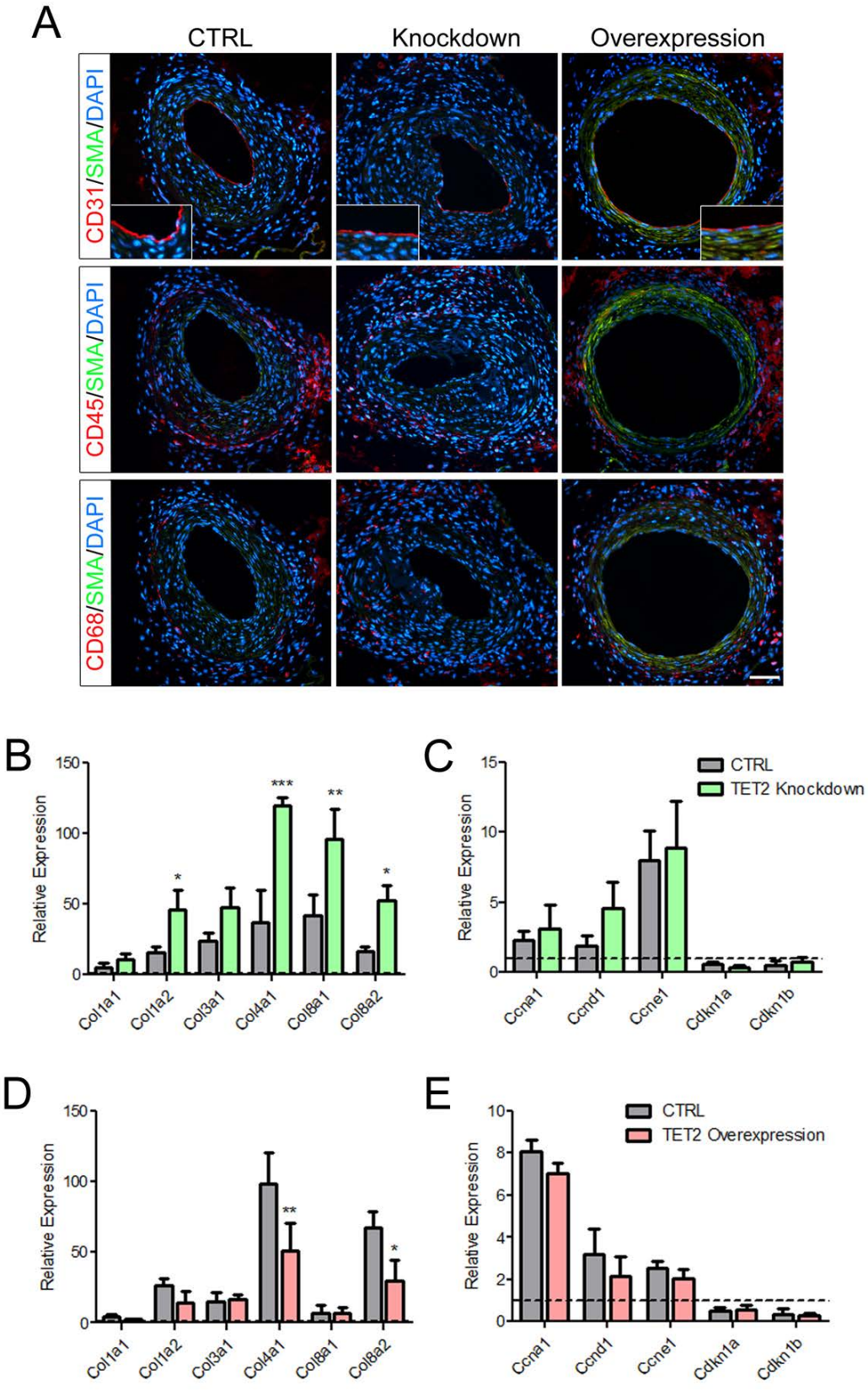
A
CTRL
Knockdown
Overexpression
CD31/SMA/DAPI
CD45/SMA/DAPI
CD68/SMA/DAPI
B
Relative Expression
Col1a1
Col1a2
Col3a1
Col4a1
Col8a1
Col8a2
C
CTRL
TET2 Knockdown
Ccna1
Ccnd1
Ccne1
Cdkn1a
Cdkn1b
D
TET2 Overexpression
E

Supplementary Figure 7: TET2 knockdown or overexpression does not affect endothelial recovery or inflammatory cell infiltration

(A) Immunofluorescence staining of CD31 (endothelial), CD45 (leukocytes) and CD68 (macrophages) on injured mouse femoral arteries that received either the control, TET2 knockdown or TET2 overexpression viruses. Scale bar = 50 μm. **(B,D)** qPCR of collagen genes in CTRL, TET2 knockdown and overexpression samples. mRNA from uninjured mouse femoral arteries was used as a reference sample and set to 1.0 (denoted by the dotted line). **(C,E)** qPCR of cyclin and cyclin dependent kinase inhibitor genes in CTRL, TET2 knockdown and overexpression samples. mRNA from uninjured mouse femoral arteries was used as a reference sample and set to 1.0 (denoted by the dotted line). mRNA was isolated and pooled together from ten sections from five individual mouse from each group. All qPCR data were normalized to *β-actin* and shown are presented as mean ± SD. $^{*}P<0.05$, $^{**}P<0.01$, $^{***}P<0.001$ relative to CTRL.

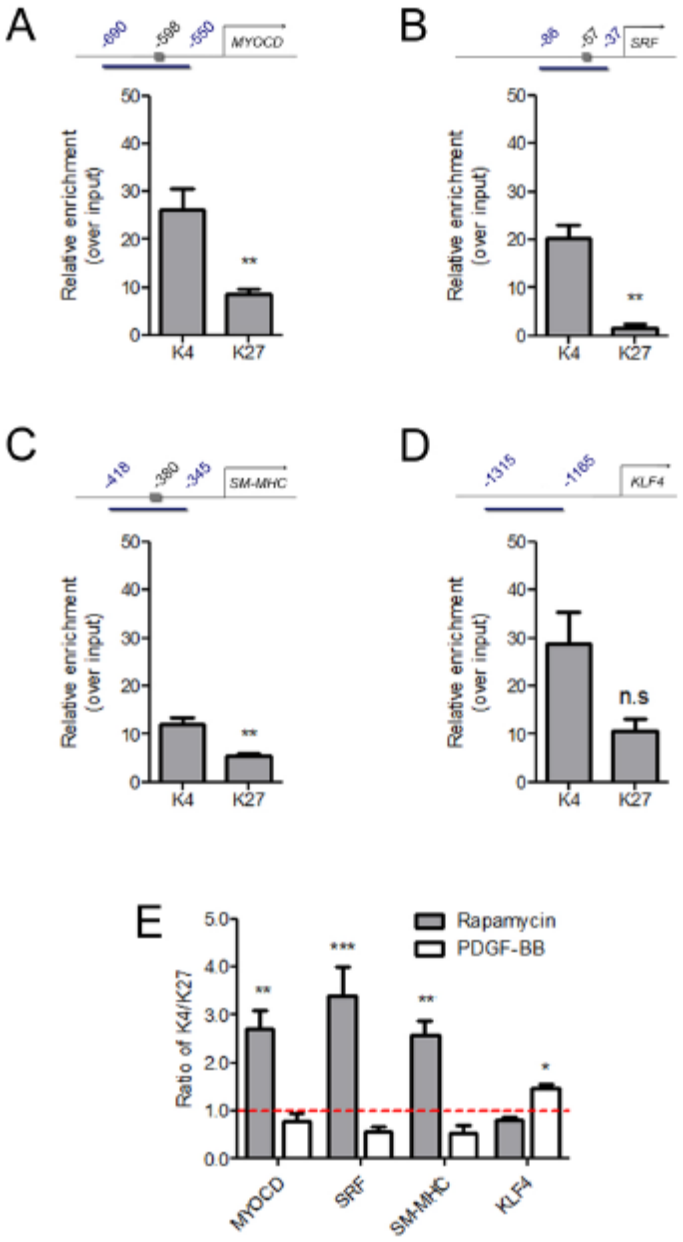

Supplementary Figure 8: Histone modification associated with SMC phenotypic plasticity

(A-D) ChIP-qPCR was performed on hCASMC with antibodies to H3K4 or H3K27 trimethylation and key promoter regions were amplified by qPCR. Data are presented as mean relative enrichment over input ± SD of four biological repeats. **(E)** H3K4 and H3K27 trimethylation ChIP-qPCR was performed on hCASMC treated with 50 nM rapamycin or 5

ng/ml PDGF-BB for 24 hours. Ratio of K4/K27 in control, untreated hCASMC is denoted by the dotted line. Primers (locations indicated by blue numbers, yielding products represented by the blue bars) were designed to encompass the CArG sequence (denoted by the gray box). Data shown are presented as mean ± SD from four independent experiments. $^{*}P<0.05$, $^{**}P<0.01$, $^{***}P<0.001$.

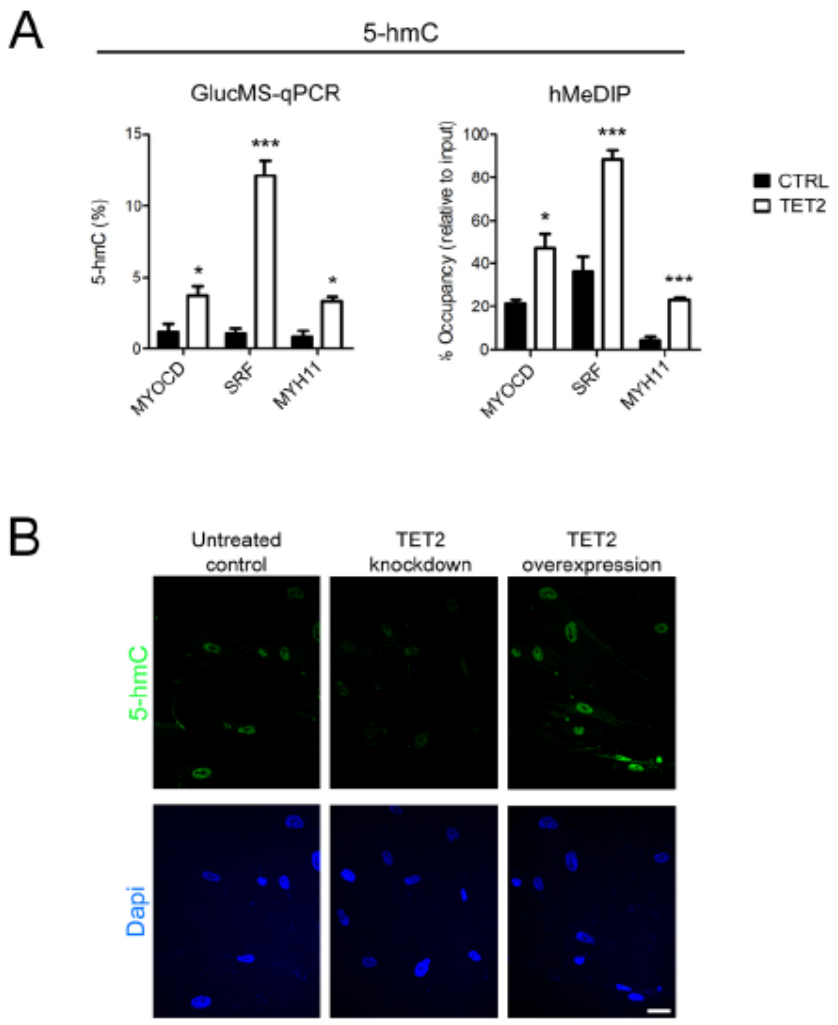

Supplementary Figure 9: TET2 regulates 5-hmC at SMC gene promoters

(**A**) 5-hmC levels in the *MYOCD*, *SRF* and *MYH11* gene promoters in TET2 overexpressing hCASMC as determined by GlucMS-qPCR or hMeDIP. (**B**) Immunocytochemistry and DAPI staining of control, TET2 knockdown and TET2 overexpressing hCASMC with an anti-5-hmC antibody. Data shown are presented as mean ± SD from four independent experiments. $^{*}P<0.01$, $^{***}P<0.001$. Scale bar, 50 μm.

Supplementary Table 1: Primers for qPCR (Human)

Primer	Forward Sequence	Reverse Sequence
β-actin	GACAGGATGCAGAAGGAGA	CCACATCTGCTGGAAGGTGG
TET1	GCAGCGTACAGGCCACCACT	AGCCGGTCGGCCATTGGAAG
TET2	TTCGCAGAAGCAGCAGTGAAGAG	AGCCAGAGACAGCGGGATTCCTT
TET3	GACGAGAACATCGGCGGCGT	GTGGCAGCGGTTGGGCTTCT
SRF*	TCACCTACCAGGTGTCGGAGTC	GTGCTGTTTGGATGGTGGAGGT
ACTA2	CAAAGCCGGCCTTACAGAG	AGCCCAGCCAAGCACTG
KLF4	GGCGGGCTGATGGGCAAGTT	TGCCGTCAGGGCTGCCTTTG
KLF5	TCGCGCGATCGGATGAGCTG	GTTGCACACCCCGCACTGGA
OPN	GGTGCATACAAGGCCATCCCCG	TCCTTCCCACGGCTGTCCCA
MYH10	ATGAGCGTCGACACGCGGAC	TGGCACGCGTCGCTTCTTCT
CCNA1	AGACCGGCTTTCCCGCAATCATGTA	TTCAGACTCCACGGGCTGCTGCTG
CCND1	CCGCAATGACCCGCACGAT	GCAACGAAGGTCTGCGCGTG
CCNE1	TGCTGGACAAAGCCCGAGCAA	TTACCGCTCTGTGGCGGGGT
CDKN1A	AGCAGGCTGAAGGGTCCCCA	CAGCCGGCGTTTGGAGTGGT
CDKN1B	AGCGACCTGCAACCGACGAT	GGCCAGGCTTCTTGGGCGTC
CDH5	CCTACCAGCCCAAAGTGTGT	GACTTGGCATCCCATTGTCT
PECAM1	GAGAGGACATTGTGCTGCAA	ATGGGGCAAGAATGACTCTG
S100A4*	CAGAACTAAAGGAGCTGCTGACC	CTTGGAAGTCCACCTCGTTGTC

MYOCD (QT00072884) and MYH11 (QT00069391) were QuantiTect primers purchased from Qiagen
* Denotes primers from Origene.

Supplementary Table 2: Primers for qPCR (Mouse)

Primer	Forward Sequence	Reverse Sequence
β-actin	GACAGGATGCAGAAGGAGA	CCACATCTGCTGGAAGGTGG
Tet1	ATGAGCGGCACCCTGAAGCG	GCACCGAGCCGTGAATGGGT
Tet2	CCTTGCATTGGAGGGGTGGCT	GTGGGGTGATTCCGGTCGGG
Tet3	CACGGCTTCGAGGCAAGCCA	CCCCGGTTCCCATCCCCCAT
Myocd	GCTGGGCTCAACCCTTGTCCC	CGTTGGCCCCACCTTGTCAGA
Srf*	CTCACCTACCAGGTGTCGGAAT	CTGCTGACTTGCATGGTGGTAG
Acta2	GTCCCAGACATCAGGGAGTAA	TCGGATACTTCAGCGTCAGGA
Myh11	AAGCTGCGGCTAGAGGTCA	CCCTCCCTTTGATGGCTGAG
Ccna1	CACCGATGATACGTACACGAAGCG	AGGAGGAACTGGTTGGTGGTTGG
Ccnd1	CGTGGTGGCTGCGATGCAAG	GTGCGTTGTGCGGTAGCAGGA
Ccne1	ACGGGTGAGGTGCTGATGCC	GCAGCCAACATCCAGGACGCA
Cdkn1a	CCACGTGGCCTTGTCGCTGT	TGCCTCCGTTTTCGGCCCTG
Cdkn1b	GCGGAGCAGTGTCCAGGGAT	GCGTCTGCTCCACAGTGCCA
Col1a1	GCCTGGACTTCCTGGTCC	AGCAAAGTTTCCTCCAAGGC
Col1a2	CTGGCATTGATGGCAGACCT	TGGGTCCAGGGAATCCAATG
Col3a1	AAATTCTGCCACCCCGAACT	AGCATCCATCTTGCAGCCTT
Col4a1	CCATGTCCATGGCACCCATC	ACCGCACACCTGTTTTCCAA
Col8a1	AGAGAAGGGCTTTGGGATGC	CTCCCGGTAGTCCAACTGGT
Col8a2	TATTACTGTCCCTGGGCTGC	GGGGCCAGAATCACCTTTGT
S100a4*	AGCTCAAGGAGCTACTGACCAG	GCTGTCCAAGTTGCTCATCACC

Myh11 (QT01060843) was QuantiTect primers purchased from Qiagen
* Denotes primers from Origene.

Supplementary Table 3: Primers for ChIP-qPCR/hMeDIP-qPCR/MethylCap

Primer	Forward Sequence	Reverse Sequence	CArG sequence	Position from TSS
MYOCD	TCTCCAGATGCGCCGTGTCA	TCAGGGCACTGGCAGAGACGA	CCAGTATTGG	-598
SRF	GTGCCGGAACCACGGAC	CTTTTATGGCGAGGCCGCT	CCATATAAGG	-57
MYH11	GTGAGTATTGCAGGCAGCCA	CTCCCAACACATTTCTAATGCCT	CCTCATAAGG	-380
KLF4	AACTTGCCCATCAGCCCGCC	CCCTCCGACGGCTCCCTTCA		

Supplementary Table 4: Primers for GlucMS-PCR

Primer	Forward Sequence	Reverse Sequence
MYOCD_MspI	AGCCTATAGACAGGCGCCCAGG	TCTGGATCTGAGCGGGGCGA
SRF_MspI	GTGCCGGAACCACGGAC	CTTTTATGGCGAGGCCGCT
MYH11_MspI	TCTGCAGACCGAGTTCCTAGA	GAATCAGACCACAACCAAGCC

References

(1) Sanburn N, Cornetta K. Rapid titre determination using quantitative real-time PCR. *Gene Therapy* 1999;6:1340-5.

(2) Sastry L, Johnson T, Hobson MJ, Smucker B, Cornetta K. Titering lentiviral vectors: comparison of DNA, RNA and marker expression methods. *Gene Therapy* 1999;2002:1155-62.

(3) Ding M, Carrao AC, Wagner RJ, Xie Y, Jin Y, Rzucidlo EM, Yu J, Li W, Tellides G, Hwa J, Aprahamian TR, Martin KA. Vascular smooth muscle cell-derived adiponectin: a paracrine regulator of contractile phenotype. *J Mol Cell Cardiol* 2012;52:474-84.

(4) Ding M, Xie Y, Wagner RJ, Jin Y, Carrao AC, Liu LS, Guzman AK, Powell RJ, Hwa J, Rzucidlo EM, Martin KA. Adiponectin induces vascular smooth muscle cell differentiation via repression of mammalian target of rapamycin complex 1 and FoxO4. *Arterioscler Thromb Vasc Biol* 2011;31:1403-10.

(5) Martin KA, Rzucidlo EM, Merenick BL, Fingar DC, Brown DJ, Wagner RJ, Powell RJ. The mTOR/p70 S6K1 pathway regulates vascular smooth muscle cell differentiation. *Am J Physiol Cell Physiol* 2004;286:C507-C517.

(6) Martin KA, Merenick BL, Ding M, Fetalvero KM, Rzucidlo EM, Kozul CD, Brown DJ, Chiu HY, Shyu M, Drapeau BL, Wagner RJ, Powell RJ. Rapamycin promotes vascular smooth muscle cell differentiation through insulin receptor substrate-1/phosphatidylinositol 3-kinase/Akt2 feedback signaling. *J Biol Chem* 2007;282:36112-20.